Monthly Variation in Flux of Inorganic Nutrients From Submarine Groundwater Discharge in a Volcanic Island: Significant Nitrogen Contamination in Groundwater

Jeonghyun Kim[1], Byung-Chan Song[1,2], Min-Young Lee[3] and Tae-Hoon Kim[3]*

[1] Department of Earth and Marine Sciences, College of Ocean Sciences, Jeju National University, Jeju City, South Korea,
[2] Jeju Groundwater Research Center, Jeju Research Institute, Jeju City, South Korea, [3] Department of Oceanography, Faculty of Earth Systems and Environmental Sciences, Chonnam National University, Gwangju, South Korea

To determine nutrient fluxes derived from submarine groundwater discharge (SGD), we conducted monthly hydrological surveys on the coast of Jeju, a volcanic island located in the southern sea of Korea. The concentrations of dissolved inorganic nitrogen (DIN), dissolved inorganic phosphorus (DIP), and dissolved silicon (DSi) were significantly correlated with salinity, indicating that fresh SGD (FSGD) is a major nutrient source in Jeju Island where no other coastal freshwater origins exist. Based on a DSi-mass balance model, seepage rate of FSGD was found to depend on 5-day precipitation before sampling campaigns, which immediately permeated *via* porous aquifers. Thus, the FSGD-driven nutrient fluxes were generally higher in rainy season (July–August) and September 2019 when typhoons occurred. However, high DIN and DIP fluxes were found during spring (March–May), even at low seepage rate, perhaps by a fertilizer input from agriculture activity. This study highlights that large variation of the SGD-driven nutrient fluxes was caused by environmental and anthropogenic factors and emphasizes on the importance of long-term investigation.

Keywords: submarine groundwater discharge, nutrient, eutrophication, Jeju, nitrogen contamination, SGD

INTRODUCTION

Submarine groundwater discharge (SGD) is the outflow of groundwater from seabed to ocean regardless of water composition or driving force (Burnett et al., 2003). Meteoric groundwater moving from land to the coastal ocean through the impervious aquifer boundaries, having low salinity groundwaters, is referred to as fresh SGD (FSGD). However, seawater can infiltrate into coastal seabed and then discharge again, to the ocean as groundwater with various ranges of salinity. This is designated as saline SGD (SSGD). Both types of SGDs flow out across the water-sediment interface at extensive coastal and marginal scales, and the advection rate was found to be as much as that from rivers. Based on previous studies, the water flux of SGD into the ocean was estimated to be similar or sometimes significantly larger than the river that acted as the major source of water. In the Atlantic Ocean, the water flux of SGD was 80–160% of the river (Moore et al., 2008). Kwon et al. (2014) estimated the SGD flux to be 3–4 times larger than the rivers in the global oceans.

Submarine groundwater discharge generally contains more enriched terrestrial substances (e.g., nutrients, organic matter, trace elements, and radionuclides) as compared to the overlying seawater (Hwang et al., 2005; Jeong et al., 2012; Kim and Kim, 2017). During the flowing and mixing of FSGD and SSGD through the underground mixing zone within a coastal aquifer, termed as the subterranean estuary (STE; Moore, 1999), intensive biogeochemical reactions modify the properties of the coastal groundwater (Beck et al., 2007; Kroeger and Charette, 2008; Anschutz et al., 2009). In addition, longer residence times of the groundwater within the STEs (hours to years), which is enriched in sedimentary organic matter, various microbial communities, water-rock interactions, and several possible electron acceptors contribute toward an increase (e.g., nitrate, ammonium, and silicate) (Mulligan and Charette, 2006; Oehler et al., 2019; Adyasari et al., 2020; Ruiz-González et al., 2021) or a decrease in the concentration of terrestrial chemicals (e.g., phosphate and nitrogen) (Kroeger and Charette, 2008). Therefore, considering the groundwater discharge rate, the SGD has been recognized as a critical process for land-sea material exchange (Beusen et al., 2013; Rodellas et al., 2015; Cho et al., 2018; Luijendijk et al., 2020).

Jeju Island was formed by multiple volcanic activities, the bedrock consists of porous basaltic rocks. Previous studies have found that permanent streams and rivers do not exist and most freshwater is discharged as groundwater into the coastal zone (Kim et al., 2003, 2011; Hwang et al., 2005). As Jeju Island is located in the southern sea of Korea on the branch of oligotrophic Kuroshio Current (Figure 1; Kim and Kim, 2017), very limited external sources of terrestrial substances are expected. However, severe benthic macroalgal blooms, commonly referred to as green tides, have been observed recently in the coastal ocean round Jeju Island. It was reported that the green tides seem to be triggered by excess nutrient loadings *via* SGD and coastal eutrophication (Kwon et al., 2017). The coastal eutrophication derived from contamination of groundwater occurs worldwide and is significantly associated with the poorly managed discharge from livestock wastewater, agricultural fertilizer, and sewage into aquifers (Laroche et al., 1997; Gobler and Sañudo-Wilhelmy, 2001; Hu et al., 2006).

The investigation of SGD with respect to seepage rate and presence of chemical substances is difficult owing to the lack of proper tools, invisible pathways under the seabed, and very large temporal and spatial variations. To overcome these problems, various geochemical tracers, e.g., ^{222}Rn, methane, silicate, and fluorescent dissolved organic matter which are usually highly enriched in the groundwater (Corbett et al., 2000; Hwang et al., 2005; Cho et al., 2021), have been used. In this study, we investigated monthly environmental factors in Hwasun Bay of Jeju Island, where the SGD is the major source of terrestrial substances, as reported in previous studies (Kim et al., 2013). Especially, the temporal scale of SGD is a key research topic to get a better insight into the understanding of variations in influence on coastal biogeochemical budget and the representative value of the SGD-driven nutrient contribution. Here, we applied the mass balance model to calculate the seepage rate and temporal variation of SGD in the coastal region. The clear variation of the SGD-driven inorganic nutrients was influenced by the hydrological environmental properties and anthropogenic activity near the study area.
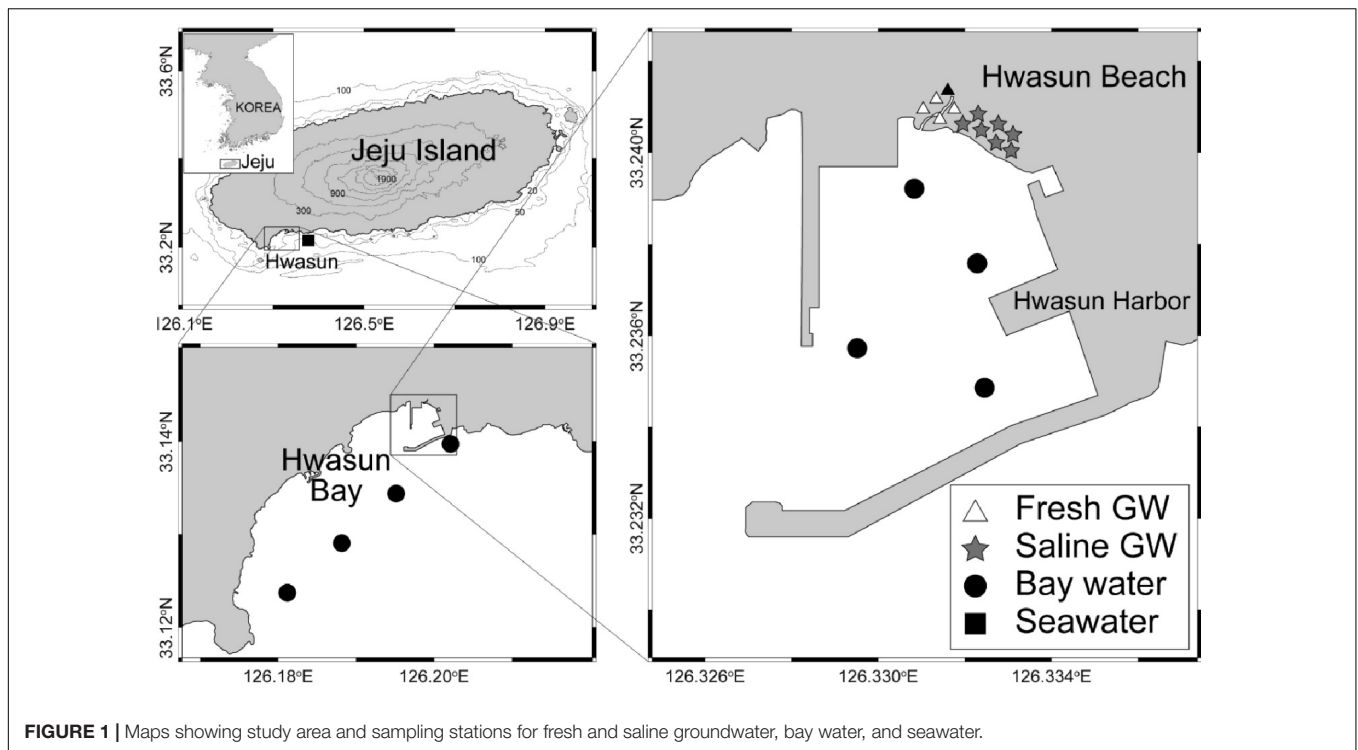
MATERIALS AND METHODS

Study Region
Jeju Island is a dormant volcanic island located in the south of the Korean Peninsula (Figure 1). As the island bedrock is mainly composed of permeable basalt rocks, it allows rainwater to recharge groundwater immediately and is transferred to the coastal region through an aquifer. Due to the influence of the East Asian monsoon climate, considerable precipitation is concentrated from June to September (mean annual precipitation ~1,900 mm). Therefore, approximately 1,000 artesian springs and wells are distributed along the coast of Jeju, and FGW provides 90% of the water resources in Jeju Island. Because Jeju Island is located on the pathway of a branch of the oligotrophic Kuroshio Current with very depleted nutrients and the SGD is a dominant source of terrestrial substances, this island is an ideal place to determine the influence of SGD-driven inorganic nutrients in the coastal ocean. The sampling campaigns were conducted in Hwasun Bay, which is in the southwest part of the island (Figure 1). The bay is semi-enclosed by beaches, rocks, and a harbor. It is well documented that FSGD is a significant process and very simple mixing pattern was observed in artesian springs, coastal groundwater, and bay water (Lee and Kim, 2015).

Sampling
The sampling campaigns were conducted monthly during 2019. To determine the effect of a typhoon on SGD, two sampling campaigns were conducted just after Typhoon *Lingling* passed (September 10 and 24, 2019). The typhoon arrived in Jeju Island on September 7 and drove record-breaking wind speeds of 54.4 m s^{-1}, the fifth most powerful in Korea's recorded history. Moreover, heavy precipitation of over 416 mm was measured in 2 days around the summit of Mt. Hallasan on Jeju Island.

The fresh and saline groundwater samples were collected in Hwasun Beach during ebb tide (Figure 1). The sampling spots were same as Kim et al. (2013) to compare with the results from the previous study. Although the spots are clustered in the small beach area, Hwasun Beach having an artesian well is the only place to take FGW samples in the bay because the outside of the beach is covered by a rocky cliff. Based on the result from hydrological survey, the lower salinity in bay water is observed near the beach area, indicating the groundwater sampling was reasonable. The FGW samples were collected near the artesian wells using a plastic beaker. The saline groundwater was sampled from shallow pits (Depth: ~50 cm) dug in beach sediments. The first two pit volumes of seeping groundwater were discarded using a plastic beaker, and the freshly recharged water was collected within the next 5 min to obtain saline groundwater samples. The salinity was measured at the sampling site using a portable sensor (CyberScan PCD650, Thermo Fisher Scientific, Waltham, MA, United States). The sensor was

FIGURE 1 | Maps showing study area and sampling stations for fresh and saline groundwater, bay water, and seawater.

calibrated using a Conductivity Standard Solution (THERMO EUTECH, Singapore) before each sampling campaign.

The surface seawater samples of bay water and its coastal area were collected aboard the R/V Je-Ra of the Jeju National University, Jeju City, South Korea. An SBE carousel water sampler (Sea-Bird Scientific, Bellevue, WA, United States) was used for the sampling of surface seawater. All water samples were collected using the 10% hydrochloric acid-cleaned Nalgene HDPE bottles.

Analysis of Inorganic Nutrients

The water samples were vacuum filtered through combusted (550°C for 4 h) Whatman glass fiber filters (GF/F, pore size: 0.7 μm) within 1 h of each sampling campaign. The filtrates were kept in a freezer (−20°C) before analysis (usually the storage duration was less than a week). Concentrations of dissolved inorganic nutrients [NO_3^-, NO_2^-, NH_4^+, PO_4^{3-}, and $Si(OH)_4$] were photometrically analyzed using an auto-analyzer (New QuAAtro39, SEAL Analytical, Southampton, United Kingdom). The accuracy of the concentration was verified before measurement of the samples using three different certified reference materials (CRM): MOOS-3 (National Research Council of Canada), RMNS (KANSO, Japan), and CSK standard solution (WAKO, Japan). Our CRM measurement results were in good agreement with the certified values (within 2%). The detection limits of NO_3^-, NO_2^-, NH_4^+, PO_4^{3-}, and $Si(OH)_4$ were 0.02, 0.04, 0.08, 0.05, and 0.06 μM, respectively. We defined the concentration of DIN as the sum of NO_3^-, NO_2^-, and NH_4^+, that of DIP as the concentration of PO_4^{3-}, and that of DSi as the concentration of $Si(OH)_4$.

RESULTS

Salinity

The salinity of the fresh groundwater (FGW) samples was constant during all sampling campaigns (avg.: 0.1 ± 0.0) (**Supplementary Table 1**). The monthly average salinities of the saline groundwater (SGW), bay water (BW), and seawater (SW) ranged from 12.9 to 18.8 (avg.: 15.5 ± 1.6), from 28.6 to 33.6 (avg.: 31.7 ± 1.6), and from 30.5 to 33.6 (avg.: 32.3 ± 0.9), respectively. The salinity values during the winter season (January, February, and December) were relatively higher than those during the summer season (June, July, and August) due to high precipitation from the East Asian monsoon.

Dissolved Inorganic Nitrogen

In the FGW, concentrations of dissolved inorganic nitrogen (DIN) ranged from 288 to 2,485 μM (avg.: 818 ± 730 μM) (**Supplementary Table 1**). The seasonal average concentrations of DIN were 1,927 ± 228 μM in spring, 300 ± 2 μM in summer, 337 ± 39 μM in autumn, and 871 ± 198 μM in winter. For the SGW, concentration of DIN ranged from 65 to 832 μM (avg.: 364 ± 274 μM). The seasonal average concentrations of DIN were 781 ± 521 μM in spring, 182 ± 54 μM in summer, 172 ± 77 μM in autumn, and 386 ± 197 μM in winter. In the BW, concentration of DIN ranged from 1.3 to 41 μM (avg.: 15.9 ± 13.7 μM). The seasonal average concentrations of DIN were 10.0 ± 17.5 μM in spring, 17.8 ± 18.0 μM in summer, 24.3 ± 30.3 μM in autumn, and 8.8 ± 10.3 μM in winter. In the SW, concentration of DIN ranged from 0.3 to 10.7 μM (avg.: 4.2 ± 4.1 μM). The seasonal average concentrations of DIN were

7.4 ± 2.9 μM in spring, 3.0 ± 3.0 μM in summer, 0.6 ± 0.2 μM in autumn, and 6.9 ± 5.3 μM in winter.

Dissolved Inorganic Phosphorus

In the FGW, concentrations of dissolved inorganic phosphorus (DIP) ranged from 2.3 to 5.8 μM (avg.: 3.7 ± 1.1 μM) (**Supplementary Table 1**). The seasonal average concentrations of DIP were 4.9 ± 0.5 μM in spring, 3.7 ± 0.4 μM in summer, 3.0 ± 0.7 μM in autumn, and 3.6 ± 0.3 μM in winter. In the SGW, concentration of DIP ranged from 1.1 to 5.2 μM (avg.: 2.8 ± 1.4 μM). The seasonal average concentrations of DIP were 4.8 ± 1.8 μM in spring, 3.2 ± 1.2 μM in summer, 1.6 ± 0.7 μM in autumn, and 2.6 ± 1.1 μM in winter. In the BW, concentration of DIP ranged from 0.3 to 0.7 μM (avg.: 0.5 ± 0.1 μM). The seasonal average concentrations of DIP were 0.6 ± 0.3 μM in spring, 0.4 ± 0.1 μM in summer, 0.5 ± 0.2 μM in autumn, and 0.5 ± 0.2 μM in winter. In the SW, concentration of DIP ranged from 0.0 to 0.7 μM (avg.: 0.2 ± 0.2 μM). The seasonal average concentrations of DIP were 0.3 ± 0.0 μM in spring, 0.1 ± 0.1 μM in summer, 0.1 ± 0.0 μM in autumn, and 0.4 ± 0.3 μM in winter.

Dissolved Silicon

In the FGW, concentrations of dissolved silicon (DSi) ranged from 158 to 566 μM (avg.: 337 ± 142 μM) (**Supplementary Table 1**). The seasonal average concentrations of DSi were 390 ± 58 μM in spring, 392 ± 83 μM in summer, 384 ± 81 μM in autumn, and 163 ± 38 μM in winter. In the SGW, concentration of DSi ranged from 97 to 269 μM (avg.: 184 ± 55 μM). The seasonal average concentrations of DSi were 217 ± 85 μM in spring, 207 ± 35 μM in summer, 195 ± 83 μM in autumn, and 115 ± 44 μM in winter. In the BW, concentration of DSi ranged from 7.7 to 30.6 μM (avg.: 15.9 ± 7.7 μM). The seasonal average concentrations of DSi were 10.4 ± 4.4 μM in spring, 20.1 ± 11.9 μM in summer, 19.8 ± 17.2 μM in autumn, and 11.9 ± 7.7 μM in winter. In the SW, concentration of DSi ranged from 3.6 to 13.0 μM (avg.: 7.2 ± 3.2 μM). The seasonal average concentrations of DSi were 6.2 ± 3.3 μM in spring, 9.9 ± 3.1 μM in summer, 4.3 ± 1.1 μM in autumn, and 9.3 ± 1.6 μM in winter.

DISCUSSION

In the FGW samples, the concentration of DSi was relatively low in the winter season and was almost constant in other seasons (**Supplementary Table 1**). The concentration of DIN was the highest in the spring season and was relatively higher in the winter season as compared to those in the summer and autumn seasons. The DIP concentration was relatively higher in the spring season as compared to those in other seasons. In particular, the DIN:DIP ratio in the FGW samples (198 ± 127) was significantly higher than that in the saline groundwater samples (124 ± 89), bay water samples (27 ± 38), and seawater samples (14 ± 12) (**Supplementary Table 2**). This indicates that the highly DIN-contaminated FGW dispersed in the bay system and potentially influenced the costal ecosystem and nitrogen budget. In the FGW, the DIN:DIP ratio was significantly higher in the spring season (342 ± 89) as compared to those in the

other seasons (118 ± 49). In the coastal regions of Jeju Island, synthetic fertilizers containing nitrogen and phosphorus are a major source of anthropogenic nutrients (Samanta et al., 2019), and the usage is concentrated in the spring season. Thus, the enriched nutrient concentrations in the FGW may originate from agricultural activities near the study region.

In general, the concentrations of inorganic nutrients in the samples from the FGW, SGW, BW, and SW were negatively correlated with salinity in all sampling campaigns (r^2 = 0.53–0.91 for DIN, 0.19–0.81 for DIP, and 0.73–0.88 for DSi; **Supplementary Figures 1–3**), indicating that the origin of freshwater increased the concentration of inorganic nutrients in the coastal Hwasun area. As there are no major rivers in Jeju Island, the freshwater must have originated from the coastal FGW. On Hwasun Beach, an artesian spring provides a large amount of FGW and creates a small stream emerging from the coastal beach. Additionally, the linear relationship between inorganic nutrients and salinity (**Supplementary Figures 1–3**) indicated the FGW-driven inorganic nutrients were likely to behave conservatively during transport into the large Hwasun Bay with little additional inputs and nutrient uptake.

Usually, the measured concentrations of the nutrients from the spring wells and shallow pits were considered to be the representative concentrations of the coastal FGW (Santos et al., 2008). Additionally, we found that these were similar to the y-intercepts of the linear relationships during most sampling campaigns (**Supplementary Figures 1–3**). However, some y-intercept values were likely to show large deviation and were out of range, particularly in the post-typhoon campaign conducted in September 24. The notable difference seems to be attributed to the various hidden pathways of the coastal aquifer and its complexity (Kim and Kim, 2017), in addition to surface runoff and non-point FGW sources derived from the typhoon event. Thus, we selected the y-intercept value between nutrient concentrations and salinity for the saline groundwater, bay water, and seawater samples in each sampling campaign as the concentrations of extrapolated zero-salinity effective end-member in the FGW (**Figure 2**, **Supplementary Figures 4, 5** and **Supplementary Table 3**) to remove any bias arising due to coastal spring wells and complex hidden pathways of the coastal aquifer (Beck et al., 2010).

To estimate seepage rate of FSGD in Hwasun Bay, the DSi mass balance model was applied. This method has been used successfully for determination of the SGD flux in the research area at a large spatial-temporal scale, where significant difference in concentration of DSi between the groundwater and coastal sea and conservative behaviors of DSi were observed (Hwang et al., 2005; Oehler et al., 2019). In Hwasun Bay, the concentration of DSi in the FGW was 18–187 times higher than that in the SW. In addition, the DSi showed a significant negative correlation with salinity (r^2 = 0.82) for FGW, SGW, bay water, and seawater (**Supplementary Figures 1–3**), suggesting the FGW-driven DSi is conservative, and additional DSi sources are negligible. In the costal system, Oehler et al. (2019) summarized various input (FGW, SGW, diffusion, runoff, rainfall, and particle dissolution) and output processes governing DSi concentrations (biological uptake, reverse weathering, and mixing). Based on the linear

correlation between DSi and salinity, the internal processes (i.e., particle dissolution, biological uptake, and reverse weathering) seem to be minor within the water residence time. With the enriched DSi concentrations in the porewater, the dissolution rate decrease (Techer et al., 2001). To exclude the addition by rainfall, we conducted water sampling after precipitation. There are no stream and river because of water permeable basalt bedrock in this bay. Here, assuming the steady-state condition in the Hwasun Bay, the DSi mass balance model was applied with two inputs (diffusion and FSGD) and one removal (water mixing) processes, as follows.

$$R_{sed}^{DSi} \times A_{Bott} + C_{FGD}^{DSi} \times A_{Bott} \times \psi_{FSGD} - C_{EX}^{DSi} \times V_S \times \lambda_{Mix} = 0$$

where R_{sed}^{DSi} is regeneration rate of DSi from sediment, A_{Bott} is the bottom area of the bay ($\times 10^7$ m^2), C_{FGD}^{DSi} is the end-member concentration of DSi in FGW (mmol m^{-3}), A_{Bott} is the bottom area of the bay ($\times 10^7$ m^2), ψ_{FSGD} is the seepage rate of FSGD (cm d^{-1}), C_{EX}^{DSi} is the excess concentration of DSi in bay water over that in the offshore (mmol m^{-3}), V_S is the water volume of bay water ($\times 10^8$ m^3), and λ_{Mix} is the exchange rate of bay water with offshore water (d^{-1}) (**Table 1**).

Diffusive flux of DSi from bottom sediments ($\times 10^7$ mmol d^{-1}) was calculated by multiplying the bottom area of Hwasun Bay and the regeneration rate of DSi (5.0 mmol m^{-2} d^{-1}; Jung and Cho, 2003; **Table 2**). C_{FGD}^{DSi} was derived from the y-intercept

of the prediction interval between DSi and salinity values of the saline groundwater, bay water, and coastal seawater (**Figure 2** and **Supplementary Table 3**).

In the bay system, the removal of DSi term was considered by the mixing of physical water with offshore water. It was calculated by multiplying C_{EX}^{DSi}, V_S, and λ_{Mix} values of each sampling campaign. The value of λ_{Mix} was determined by a reciprocal of water residence time ($\tau_{bw} = 1/\lambda_{Mix}$). The value of τ_{bw} for each sampling campaign was calculated by the tidal prism method (Sanford et al., 1992; Moore et al., 2006; **Table 1**). Owing to high current velocity along the coastal Jeju Island (10–15 cm s^{-1}; Chang et al., 2000), the return flow effect was considered to be negligible. The residence times of the bay were lowest in February 2019 (1.4 day) and highest in September 24 (4.0 day), and the average was 2.2 ± 0.8 day, similar to the previous study using the Rn-222 mass balance model [2.5 day; Kim et al. (2011)]. Thus, the result of our estimation is reasonable.

As a result of the DSi mass balance model, the ψ_{FSGD} ranged from 1.3 cm d^{-1} in June 2019 to 22.5 cm d^{-1} in August 2019 (avg.: 6.7 ± 6.6 cm d^{-1}; **Table 1** and **Supplementary Figure 6**). During January to July and November to December 2019, the seepage rate of FSGD remained relatively low and constant at 3.0 ± 1.1 cm d^{-1}. High seepage rates were observed from August to October 2019, along with a relatively high precipitation rate (**Supplementary Figure 6**). Typically, the East Asian Monsoon lasts from July to August in the Korean Peninsula. In September 2019, precipitation of 502.8 mm was recorded in Jeju Island,
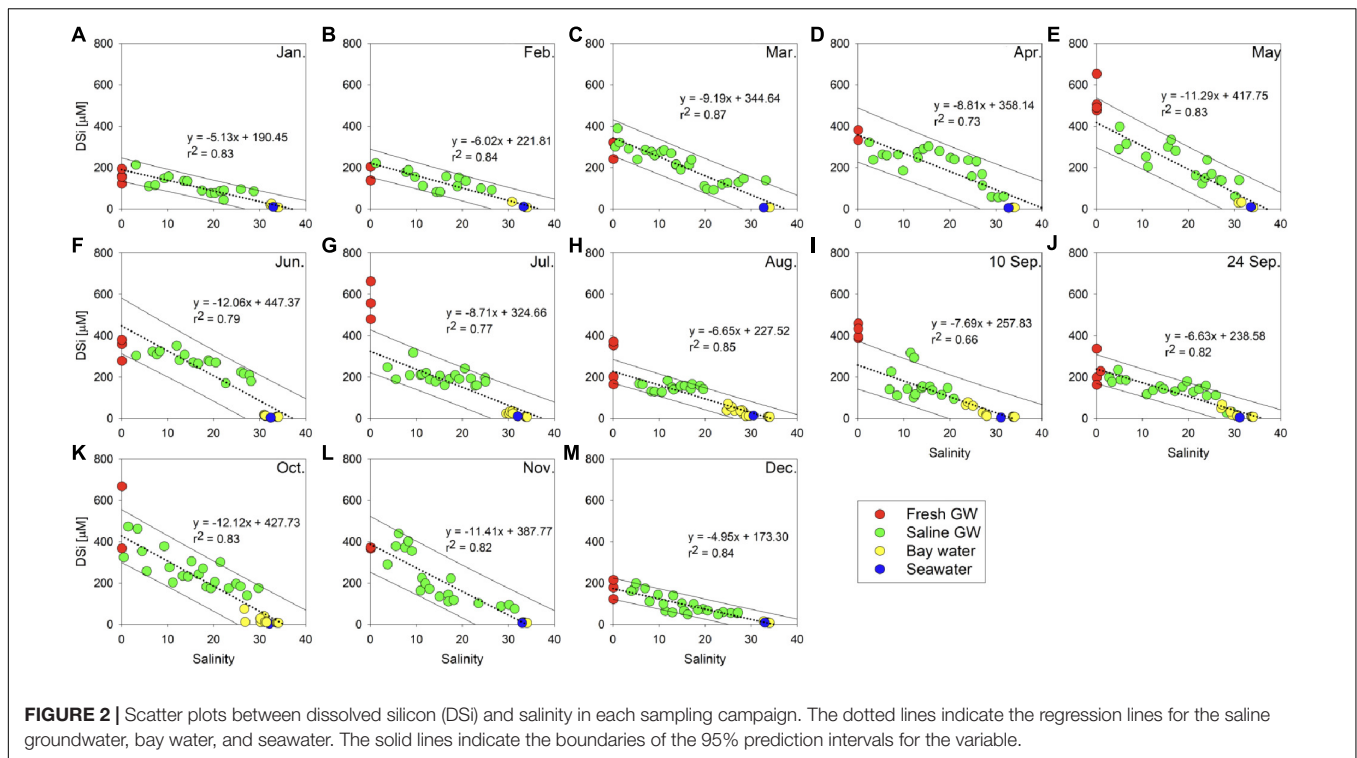
TABLE 1 | Values for each notation in the dissolved silicon (DSi) mass balance model in Hwasun Bay, Jeju Island.

Value (unit)	January	February	March	April	May	June	July	August	September 10	September 24	October	November	December
F_{Diff} ($\times 10^7$ mmol d^{-1})	9.5	9.5	9.5	9.5	9.5	9.5	9.5	9.5	9.5	9.5	9.5	9.5	9.5
C_{FGW} (mmol m^{-3})	190	222	345	358	418	447	325	228	258	239	428	388	173
A_{bott} ($\times 10^7$ m^2)	1.9	1.9	1.9	1.9	1.9	1.9	1.9	1.9	1.9	1.9	1.9	1.9	1.9
C_{EX} (mmol m^{-3})	3.5	2.3	4.1	2.6	5.0	4.0	6.7	17.6	25.3	17.4	16.3	2.7	2.0
V_s ($\times 10^8$ m^3)	1.3	1.5	1.5	1.5	1.3	1.3	1.3	1.1	1.3	1.3	1.4	1.5	1.5
τ_{bw} (day)	2.6	1.4	1.5	1.6	1.9	2.6	2.6	1.8	3.5	4.0	2.6	1.6	1.5
λ_{Mix} (d^{-1})	0.39	0.70	0.68	0.64	0.52	0.39	0.39	0.56	0.28	0.25	0.39	0.61	0.67
Ψ (cm d^{-1})	2.5	3.6	4.9	2.3	3.2	1.3	4.1	22.5	17.6	10.5	9.4	2.0	3.0

F_{Diff} is the diffusive flux, C_{FGW} is the end-member of DSi concentration in fresh groundwater, A_{bott} is bottom area of the bay, C_{EX} is the excess concentration of DSi in bay water over that in the offshore, V_S is the water volume of bay water, τ_{bw} is residence time of bay water, λ_{Mix} is the exchange rate of bay water with the offshore water, and Ψ is the seepage rate of the FSGD.

TABLE 2 | The summaries of the geochemical tracer based fresh submarine groundwater discharge (FSGD) estimates and the associated nutrient fluxes to the coastal zones of volcanic islands (Jeju and Hawaii).

Study region	FSGD rate	Length	DIN flux	DIP flux	DSi flux	Tracers	References
	m^3 d^{-1}	m	mol yr^{-1}				
Kona, Hawaii	6.7–13 $\times 10^5$	8,320	2.4–5.4 $\times 10^7$	1.6–2.9 $\times 10^6$	2.4–4.5 $\times 10^8$	Ra	Knee et al., 2010
Kuau	11,200	2,946	1.8 $\times 10^6$	2.0 $\times 10^4$	3.6 $\times 10^6$	Rn	Bishop et al., 2017
Maalaea	6,430	1,568	6.8 $\times 10^5$	1.7 $\times 10^4$	1.4 $\times 10^6$	Rn	Bishop et al., 2017
Kahului	3,030	2,754	6.1 $\times 10^4$	2.6 $\times 10^3$	7.3 $\times 10^5$	Rn	Bishop et al., 2017
Honolua	4,670	1,061	4.9 $\times 10^4$	2.9 $\times 10^3$	8.1 $\times 10^5$	Rn	Bishop et al., 2017
Waiehu	626	1,252	8.4 $\times 10^3$	7.3 $\times 10^2$	1.2 $\times 10^5$	Rn	Bishop et al., 2017
Honomanu	3,020	1,043	8.8 $\times 10^3$	3.7 $\times 10^3$	7.5 $\times 10^5$	Rn	Bishop et al., 2017
Hwasun Bay	1.3 ± 1.3 $\times 10^6$	8,700	2.1 ± 1.4 $\times 10^8$	1.4 ± 0.7 $\times 10^6$	1.3 ± 1.1 $\times 10^8$	DSi	This study

FIGURE 2 | Scatter plots between dissolved silicon (DSi) and salinity in each sampling campaign. The dotted lines indicate the regression lines for the saline groundwater, bay water, and seawater. The solid lines indicate the boundaries of the 95% prediction intervals for the variable.
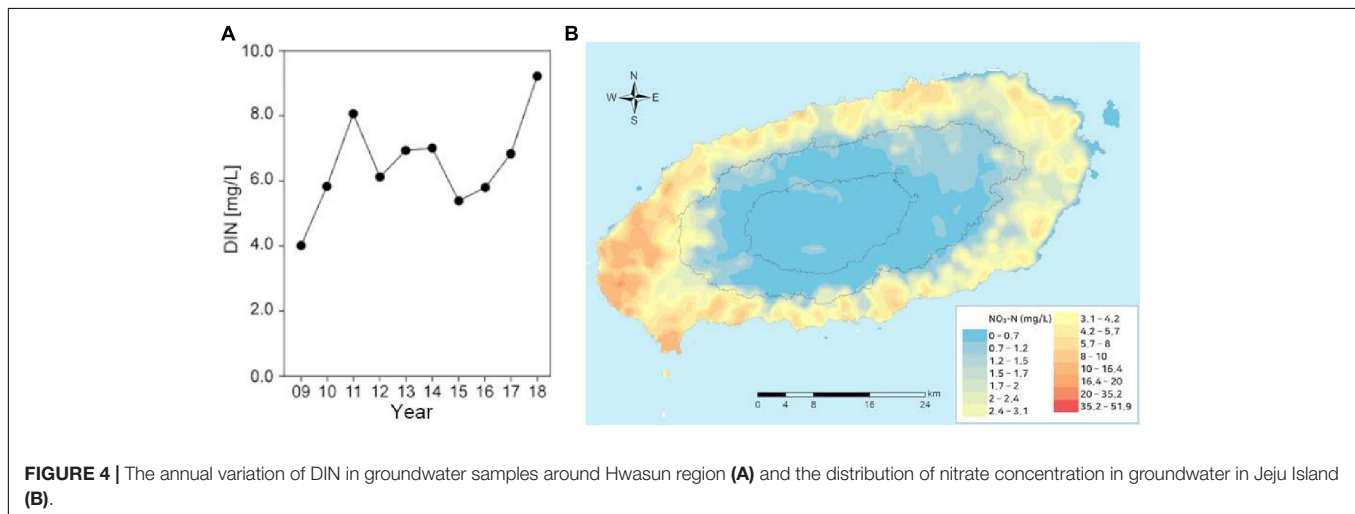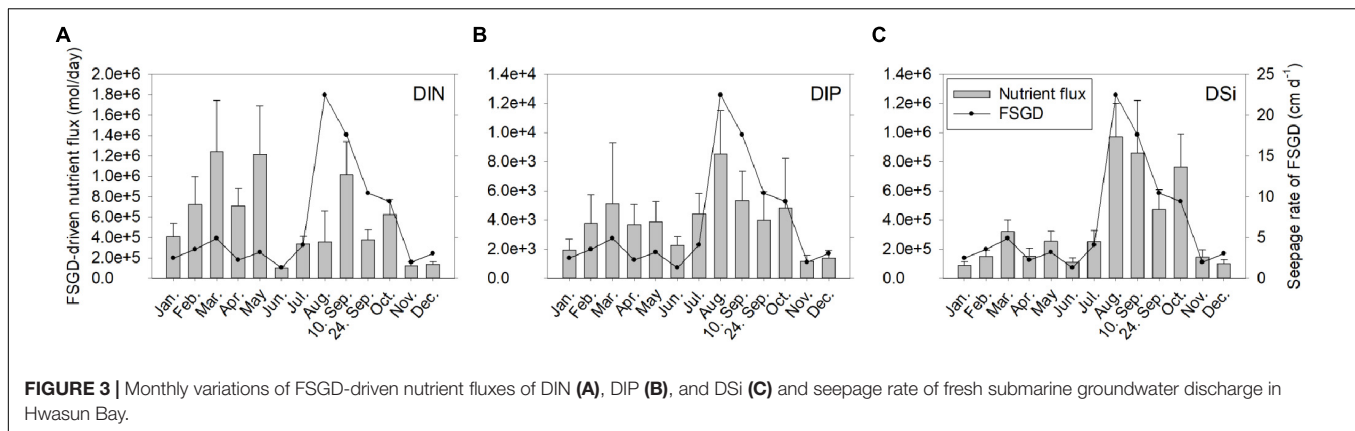
which was significantly higher than the average range of monthly precipitation (113.6 mm to 243.1 mm), perhaps owing to frequent typhoon events (Typhoons *Lingling*, *Tapah*, and *Mitag*). On both sampling campaigns in September 2019, a heavy precipitation was recorded after Typhoon *Lingling*, and relatively high seepage rates were observed (17.6 cm d^{-1} for September 10 and 10.5 cm d^{-1} for September 24). Therefore, the transport of groundwater *via* the SGD in Hwasun Bay was significantly increased by heavy precipitation from the East Asian Monsoon and the typhoons (Cho et al., 2021). In addition, we found that the variations in the seepage rate of FSGD resembled the variations in precipitation for 5 days before each sampling campaign ($r^2 = 0.67$), rather than the monthly variations in precipitation ($r^2 = 0.31$) (**Supplementary Figure 6** and **Supplementary Table 4**). This indicates that the seepage rate of FSGD in Jeju Island seems to respond to immediate precipitation. The porous basaltic land is likely to aid rapid permeation of the precipitation into the aquifer. It is supported by the result from Cho et al. (2021). They found almost double the SGD flux (9.7×10^6 m^3 d^{-1}) in 1 day after a typhoon event compared to before the typhoon event (5.7×10^6 m^3 d^{-1}). However, in 4 days after the typhoon, the SGD flux was back to normal (4.9×10^6 m^3 d^{-1}). Thus, recent climate and weather conditions are important factors affecting the SGD rate in Jeju Island.

Santos et al. (2021) reported that although the contribution of FGW discharge to the global ocean is relatively minor compared with rivers and total SGD (less than 1%). However, the input of FGW is considerable in certain environment including the volcanic island where precipitation, permeability, and hydraulic heads are high and surface runoff is minor (Moosdorf et al., 2015;

Zhou et al., 2018, 2019). The average discharge rate of FSGD in this study ($1.3 \pm 1.3 \times 10^6$ m^3 d^{-1}) was similar with that in Kona, Hawaii [**Table 2**; Knee et al. (2010)]. Here, considering the similar coastal length of research area in Kona coast [8,320 m, Knee et al. (2010)] and Hwasun Bay (8,700 m), the seepage rate per unit length seems to be comparable in both volcanic environments.

The fluxes of inorganic nutrients *via* FSGD were calculated by multiplying the seepage rate of FSGD by the end-member concentration of nutrients in the FGW. The fluxes of DIN, DIP, and DSi ranged from 1.0×10^5 mol d^{-1} to 12×10^5 mol d^{-1} (avg.: $5.7 \pm 4.0 \times 10^5$ mol d^{-1}), from 1.2×10^3 mol d^{-1} to 8.5×10^3 mol d^{-1} (avg.: $3.9 \pm 2.0 \times 10^3$ mol d^{-1}), and from 0.9×10^5 mol d^{-1} to 9.7×10^5 mol d^{-1} (avg.: $3.6 \pm 3.1 \times 10^5$ mol d^{-1}), respectively (**Figure 3** and **Table 2**). As shown in **Figure 3**, significantly large variations of nutrient fluxes were found, and those were generally higher during the East Asian Monsoon rainy season (July–August) and September 2019, when the three typhoons arrived. The maximum fluxes of DIP and DSi were observed in August, corresponding to the largest seepage rate of FSGD. Here, the monthly precipitation in August was less than those of July and September, but the total precipitation for 5 days just before the sampling campaigns was relatively higher. We concluded that as the FSGD was affected by immediate precipitation, the nutrient fluxes may have been enriched directly in August 2019.

However, very high fluxes of DIN *via* FSGD were found during spring season (March–May), even for low seepage rates (**Figure 3**). The higher fluxes were controlled by the four times increase of end-member concentration in the FGW, which may be attributed to the nutrient contamination due to excess

FIGURE 3 | Monthly variations of FSGD-driven nutrient fluxes of DIN **(A)**, DIP **(B)**, and DSi **(C)** and seepage rate of fresh submarine groundwater discharge in Hwasun Bay.

FIGURE 4 | The annual variation of DIN in groundwater samples around Hwasun region **(A)** and the distribution of nitrate concentration in groundwater in Jeju Island **(B)**.

agricultural activities in the spring season. However, the trend of DSi was similar to that of the FSGD, indicating that the DSi was a reliable tracer for FSGD.

To compare with the other origins of nutrients, the diffusive fluxes from the bottom sediment were considered. Previous studies found that the diffusive fluxes of DIN, DIP, and DSi per square meter in this bay were 1.3, 0.6, and 5.0 mmol m^{-2} d^{-1}, respectively (Kim and Park, 1998; Jung and Cho, 2003). By multiplying the area of the Hwasun Bay, the nutrient fluxes of DIN, DIP, and DSi by diffusion at the sediment-water interface were 2.5×10^4, 1.1×10^4, and 9.5×10^4, respectively. As compared to diffusion, the FSGD-driven DIN and DSi were 23 and 3.8 times higher in Hwasun Bay, respectively, although the contribution of diffusive DIP flux was significantly higher than that of the FSGD. Although atmospheric deposition may affect the nutrient budget in the bay, there was a linear relationship between inorganic nutrients and salinity (**Supplementary Figures 1–3**), suggesting no significant external origins (e.g., *in situ* remineralization from organic matter). In addition, in a previous study, Kim et al. (2011) reported that the atmospheric deposition was negligible in Hwasun Bay.

The SGD-driven DIN flux in Hwasun Bay almost doubled in 10 years. In a previous study, the DIN flux *via* SGD in 2010–2011 was reported to be 2.9×10^5 mol d^{-1} (Kim et al., 2013), which is approximately half the value determined in this study ($5.7 \pm 4.0 \times 10^5$ mol d^{-1}). The seepage rate of SGD (FSGD + RSGD) in the same study was twice (2.2×10^6 m^3 d^{-1}) the value obtained in this study (1.3×10^6 m^3 d^{-1}). Despite the large uncertainties in the estimate, the result is supported by that the nitrogen contamination in coastal groundwater is increasing (**Figure 4A**). The groundwater in the western part of Jeju Island showed enriched nitrate-nitrogen (NO_3-N) concentration (**Figure 4B**). The nitrogen contamination may be caused by contamination from excessive use of a liquefied and chemical fertilizer in many farms (tangerine orchards and vegetable farms) distributed near Hwasun Bay based on the previous nitrogen isotopic signal ($\delta^{15}N = \sim 4.5\%_0$) (Woo et al., 2001). Especially, the isotope ratio of highly contaminated groundwater (>10 mg/L) was less than 4 ‰, indicating the anthropogenic fertilizer [-4 to $+4\%_0$, Kendall (1998)] is a major source of nitrogen contaminant (Woo et al., 2001). The coastal nitrogen contamination derived from the excessive use of nitrogen fertilizer and associated with severe hypoxic events were also reported in the Gulf of Mexico (Meter et al., 2018). They highlighted legacy nutrients can last at least 1 year beyond initial use within a watershed and remain much longer within groundwater system (Meter et al., 2018).

The nutrient pollution can be accumulated in aquifer and the purification is much difficult than river and lake systems. Therefore, the long-term monitoring and management strategies of groundwater qualities should be taken to understand the link of environmental problems and groundwater qualities.

CONCLUSION

The concentrations of DIN, DIP, and DSi were measured monthly in the FGW, SGW, bay water, and coastal seawater in Hwasun Bay of Jeju Island. The concentrations of DIN, DIP, and DSi were significantly correlated with salinity, indicating that the FSGD is a dominant source of nutrients in the bay, where no other freshwater origins exist. Based on the DSi-mass balance model, the monthly variation in the seepage rate of FSGD was significantly correlated with the accumulated precipitation that occurred for 5 days before the sampling campaigns, rather than the monthly total precipitation rate, owing to immediate influence of precipitation which flows through a porous aquifer in Jeju Island. In general, the nutrient fluxes were observed to be higher in the East Asian Monsoon rainy season and September 2019, when the three typhoons arrived (*Lingling*, *Tapah*, and *Mitag*). The very high DIN and DIP fluxes during spring season, even for low seepage rate, can be attributed to the nutrient contamination in the coastal groundwater perhaps by a fertilizer input from agriculture activity. The large variation of the SGD-driven nutrient fluxes seems to be derived from precipitation and anthropogenic activities near the study region. This study suggests that a long-term investigation is required to estimate the representative values of the seepage rate of SGD and the fluxes of terrestrial substances to cover various environmental and anthropogenic factors during different seasons. In addition, further studies will be necessary to trace the origin of the excess concentration of nitrogen during spring season, based on chemical tracers such as nitrogen isotopes.

REFERENCES

Adyasari, D., Hassenrück, C., Montiel, D., and Dimova, N. (2020). Microbial community composition across a coastal hydrological system affected by submarine groundwater discharge (SGD). *PLoS One* 15:e0235235. doi: 10.1371/journal.pone.0235235

Anschutz, P., Smith, T., Mouret, A., Deborde, J., Bujan, S., Poirier, D., et al. (2009). Tidal sands as biogeochemical reactors. *Estuar. Coast. Shelf Sci.* 84, 84–90.

Beck, A. J., Cochran, J. K., and Sañudo-Wilhelmy, S. A. (2010). The distribution and speciation of dissolved trace metals in a shallow subterranean estuary. *Mar. Chem.* 121, 145–156.

Beck, A. J., Tsukamoto, Y., Tovar-Sanchez, A., Huerta-Diaz, M., Bokuniewicz, H. J., and Sañudo-Wilhelmy, S. A. (2007). Importance of geochemical transformations in determining submarine groundwater discharge-derived trace metal and nutrient fluxes. *Appl. Geochem.* 22, 477–490. doi: 10.1016/j.apgeochem.2006.10.005

Beusen, A. H. W., Slomp, C. P., and Bouwman, A. F. (2013). Global land–ocean linkage: direct inputs of nitrogen to coastal waters via submarine groundwater discharge. *Environ. Res. Lett.* 8:034035.

Bishop, J. M., Glenn, C. R., Amato, D. W., and Dulai, H. (2017). Effect of land use and groundwater flow path on submarine groundwater discharge nutrient flux. *J. Hydrol. Reg. Stud.* 11, 194–218.

DATA AVAILABILITY STATEMENT

The original contributions presented in the study are included in the article/**Supplementary Material**, further inquiries can be directed to the corresponding author.

AUTHOR CONTRIBUTIONS

T-HK conceived and designed this study. JK performed the statistical data analysis. B-CS and M-YL contributed to the sample collection, the chemical measurement of inorganic nutrients, and the calculation of the seepage rate, and nutrient fluxes using the DSi mass balance model under the supervision of T-HK. JK and T-HK wrote the manuscript. All authors contributed to the article and approved the submitted version.

FUNDING

ACKNOWLEDGMENTS

SUPPLEMENTARY MATERIAL

The Supplementary Material for this article can be found online at: https://www.frontiersin.org/articles/10.3389/fmars.2022.835207/full#supplementary-material

Burnett, W. C., Bokuniewicz, H., Huettel, M., Moore, W. S., and Taniguchi, M. (2003). Groundwater and pore water inputs to the coastal zone. *Biogeochemistry* 66, 3–33.

Chang, K.-I., Suk, M.-S., Pang, I.-C., and Teague, W. J. (2000). Observations of the Cheju current. *J. Korean Soc. Oceanogr.* 35, 129–152.

Cho, H.-M., Kim, G., Kwon, E. Y., Moosdorf, N., Garcia-Orellana, J., and Santos, I. R. (2018). Radium tracing nutrient inputs through submarine groundwater discharge in the global ocean. *Sci. Rep.* 8:2439. doi: 10.1038/s41598-018-20806-2

Cho, H.-M., Kim, T.-H., Moon, J.-H., Song, B.-C., Hwang, D.-W., Kim, T., et al. (2021). Estimating submarine groundwater discharge in Jeju volcanic island (Korea) during a typhoon (Kong-rey) using humic-fluorescent dissolved organic matter-Si mass balance. *Sci. Rep.* 11:941. doi: 10.1038/s41598-020-79381-0

Corbett, D. R., Dillon, K., Burnett, W., and Chanton, J. (2000). Estimating the groundwater contribution into Florida Bay via natural tracers, ^{222}Rn and CH_4. *Limnol. Oceanogr.* 45, 1546–1557. doi: 10.4319/lo.2000.45.7.1546

Gobler, C. J., and Sañudo-Wilhelmy, S. A. (2001). Temporal variability of groundwater seepage and brown tide blooms in a Long Island embayment. *Mar. Ecol. Prog. Ser.* 217, 299–309.

Hu, C., Muller-Karger, F. E., and Swarzenski, P. W. (2006). Hurricanes, submarine groundwater discharge, and Florida's red tides. *Geophys. Res. Lett.* 33: L11601.

Hwang, D., Lee, Y.-W., and Kim, G. (2005). Large submarine groundwater discharge and benthic eutrophication in Bangdu Bay on volcanic Jeju Island, Korea. *Limnol. Oceanogr.* 50, 1393–1403. doi: 10.4319/lo.2005.50.5.1393

Jeong, J., Kim, G., and Han, S. (2012). Influence of trace element fluxes from submarine groundwater discharge (SGD) on their inventories in coastal waters off volcanic island, Jeju, Korea. *Appl. Geochem.* 27, 37–43. doi: 10.1016/j. apgeochem.2011.08.014

Jung, H.-Y., and Cho, K.-J. (2003). SOD and inorganic nutrient fluxes from sediment in the downstream of the Nagdong River. *Korean J. Ecol. Environ.* 36, 322–335.

Kendall, C. (1998). "Chapter 16 – tracing nitrogen sources and cycling in catchments," in *Isotope Tracers in Catchment Hydrology*, eds C. Kendall and J. J. Mcdonnell (Amsterdam: Elsevier), 519–576. doi: 10.1016/b978-0-444-81546-0.50023-9

Kim, D., and Park, C. (1998). Estimation of nutrients released from sediments of Deukryang Bay. *J. Korean Environ. Sci. Soc.* 7, 425–431.

Kim, G., Kim, J.-S., and Hwang, D.-W. (2011). Submarine groundwater discharge from oceanic islands standing in oligotrophic oceans: implications for global biological production and organic carbon fluxes. *Limnol. Oceanogr.* 56, 673–682. doi: 10.4319/lo.2011.56.2.0673

Kim, G., Lee, K.-K., Park, K.-S., Hwang, D.-W., and Yang, H.-S. (2003). Large submarine groundwater discharge (SGD) from a volcanic island. *Geophys. Res. Lett.* 30:2098.

Kim, J., and Kim, G. (2017). Inputs of humic fluorescent dissolved organic matter via submarine groundwater discharge to coastal waters off a volcanic island (Jeju, Korea). *Sci. Rep.* 7:7921. doi: 10.1038/s41598-017-08518-5

Kim, T.-H., Kwon, E., Kim, I., Lee, S.-A., and Kim, G. (2013). Dissolved organic matter in the subterranean estuary of a Volcanic Island, Jeju: importance of dissolved organic nitrogen fluxes to the ocean. *J. Sea Res.* 78, 18–24.

Knee, K. L., Street, J. H., Grossman, E. E., Boehm, A. B., and Paytan, A. (2010). Nutrient inputs to the coastal ocean from submarine groundwater discharge in a groundwater-dominated system: relation to land use (Kona coast, Hawaii, U.S.A.). *Limnol. Oceanogr.* 55, 1105–1122. doi: 10.4319/lo.2010.55.3.1105

Kroeger, K., and Charette, M. (2008). Nitrogen biogeochemistry of submarine groundwater discharge. *Limnol. Oceanogr.* 53:1025. doi: 10.4319/lo.2008.53.3.1025

Kwon, E. Y., Kim, G., Primeau, F., Moore, W. S., Cho, H. M., Devries, T., et al. (2014). Global estimate of submarine groundwater discharge based on an observationally constrained radium isotope model. *Geophys. Res. Lett.* 41, 8438–8444. doi: 10.1002/2014gl061574

Kwon, H. K., Kang, H., Oh, Y. H., Park, S. R., and Kim, G. (2017). Green tide development associated with submarine groundwater discharge in a coastal harbor, Jeju, Korea. *Sci. Rep.* 7:6325. doi: 10.1038/s41598-017-06711-0

Laroche, J., Nuzzi, R., Waters, R., Wyman, K., Falkowski, P., and Wallace, D. (1997). Brown tide blooms in long Island's coastal waters linked to interannual variability in groundwater flow. *Glob. Change Biol.* 3, 397–410. doi: 10.1046/j.1365-2486.1997.00117.x

Lee, J., and Kim, G. (2015). Dependence of pH in coastal waters on the adsorption of protons onto sediment minerals. *Limnol. Oceanogr.* 60, 831–839. doi: 10.1002/lno.10057

Luijendijk, E., Gleeson, T., and Moosdorf, N. (2020). Fresh groundwater discharge insignificant for the world's oceans but important for coastal ecosystems. *Nat. Commun.* 11:1260. doi: 10.1038/s41467-020-15064-8

Meter, K. J. V., Cappellen, P. V., and Basu, N. B. (2018). Legacy nitrogen may prevent achievement of water quality goals in the Gulf of Mexico. *Science* 360, 427–430. doi: 10.1126/science.aar4462

Moore, W. S. (1999). The subterranean estuary: a reaction zone of ground water and sea water. *Mar. Chem.* 65, 111–125. doi: 10.1016/s0304-4203(99)00014-6

Moore, W. S., Blanton, J. O., and Joye, S. B. (2006). Estimates of flushing times, submarine groundwater discharge, and nutrient fluxes to Okatee Estuary, South Carolina. *J. Geophys. Res.* 111:C09006.

Moore, W. S., Sarmiento, J. L., and Key, R. M. (2008). Submarine groundwater discharge revealed by [228]Ra distribution in the upper Atlantic Ocean. *Nat. Geosci.* 1, 309–311. doi: 10.1038/ngeo183

Moosdorf, N., Stieglitz, T., Waska, H., Dürr, H. H., and Hartmann, J. (2015). Submarine groundwater discharge from tropical islands: a review. *Grundwasser* 20, 53–67. doi: 10.1007/s00767-014-0275-3

Mulligan, A. E., and Charette, M. A. (2006). Intercomparison of submarine groundwater discharge estimates from a sandy unconfined aquifer. *J. Hydrol.* 327, 411–425. doi: 10.1016/j.jhydrol.2005.11.056

Oehler, T., Tamborski, J., Rahman, S., Moosdorf, N., Ahrens, J., Mori, C., et al. (2019). DSi as a tracer for submarine groundwater discharge. *Front. Mar. Sci.* 6:563.

Rodellas, V., Garcia-Orellana, J., Masqué, P., Feldman, M., and Weinstein, Y. (2015). Submarine groundwater discharge as a major source of nutrients to the Mediterranean Sea. *Proc. Natl. Acad. Sci. U.S.A.* 112, 3926–3930. doi: 10.1073/pnas.1419049112

Ruiz-González, C., Rodellas, V., and Garcia-Orellana, J. (2021). The microbial dimension of submarine groundwater discharge: current challenges and future directions. *FEMS Microbiol. Rev.* 45:fuab010. doi: 10.1093/femsre/fuab010

Samanta, P., Shin, S., Jang, S., Song, Y.-C., Oh, S., and Kim, J. K. (2019). Stable carbon and nitrogen isotopic characterization and tracing nutrient sources of Ulva blooms around Jeju coastal areas. *Environ. Pollut.* 254:113033. doi: 10.1016/j.envpol.2019.113033

Sanford, L. P., Boicourt, W. C., and Rives, S. R. (1992). Model for estimating tidal flushing of small embayments. *J. Waterway Port Coast. Ocean* 118, 635–654. doi: 10.1061/(asce)0733-950x(1992)118:6(635)

Santos, I. R. S., Burnett, W. C., Chanton, J., Mwashote, B., Suryaputra, I. G. N. A., and Dittmar, T. (2008). Nutrient biogeochemistry in a Gulf of Mexico subterranean estuary and groundwater-derived fluxes to the coastal ocean. *Limnol. Oceanogr.* 53, 705–718. doi: 10.4319/lo.2008.53.2.0705

Santos, I. R., Chen, X., Lecher, A. L., Sawyer, A. H., Moosdorf, N., Rodellas, V., et al. (2021). Submarine groundwater discharge impacts on coastal nutrient biogeochemistry. *Nat. Rev. Earth Environ.* 2, 307–323. doi: 10.1016/j.marpolbul.2013.07.045

Techer, I., Advocat, T., Lancelot, J., and Liotard, J.-M. (2001). Dissolution kinetics of basaltic glasses: control by solution chemistry and protective effect of the alteration film. *Chem. Geol.* 176, 235–263. doi: 10.1016/s0009-2541(00)00400-9

Woo, N.-C., Kim, H.-D., Lee, K.-S., Park, W.-B., Koh, G.-W., and Moon, Y.-S. (2001). Interpretation of groundwater system and contamination by water-quality monitoring in the Daejung Watershed, Jeju Island. *Econ. Environ. Geol.* 34, 485–498.

Zhou, Y., Befus, K. M., Sawyer, A. H., and David, C. H. (2018). Opportunities and challenges in computing fresh groundwater discharge to continental coastlines: a multimodel comparison for the United States Gulf and Atlantic Coasts. *Water Resour. Res.* 54, 8363–8380. doi: 10.1029/2018wr023126

Zhou, Y., Sawyer, A. H., David, C. H., and Famiglietti, J. S. (2019). Fresh submarine groundwater discharge to the near-global coast. *Geophys. Res. Lett.* 46, 5855–5863. doi: 10.1029/2019gl082749